PHYSICAL REVIEW E **77**, 065601(R) (2008)

Surface breathers in discrete magnetic metamaterials

Nikos Lazarides,[1,2] George P. Tsironis,[1] and Yuri S. Kivshar[3]
[1]*Department of Physics, University of Crete, and Institute of Electronic Structure and Laser, Foundation for Research and Technology–Hellas, P.O. Box 2208, 71003 Heraklion, Greece*
[2]*Department of Electrical Engineering, Technological Educational Institute of Crete, P.O. Box 140, Stavromenos, 71500 Heraklion, Crete, Greece*
[3]*Nonlinear Physics Center, Research School of Physical Sciences and Engineering, Australian National University, Canberra, ACT 0200, Australia*

(Received 17 March 2008; published 3 June 2008)

We analyze the properties of discrete breathers excited near the edge of a one-dimensional metamaterial created by a truncated array of nonlinear split-ring resonators. We study a crossover between nonlinear surface states and discrete breathers by analyzing the modes centered at finite distances from the array edge and demonstrate the existence of a class of nonlinear localized surface states, the so-called nonlinear Tamm states or *surface breathers*, which exhibit features that have no counterparts either in the continuous systems or in linear arrays.

DOI: 10.1103/PhysRevE.77.065601 PACS number(s): 41.20.Jb, 63.20.Pw, 75.30.Kz, 78.20.Ci

It is well established that a special class of localized modes can be generated at surfaces, and such surface states have been studied in many areas of physics including electrons in crystals [1,2], surface phonons [3], and surface polaritons [4]. Recently, the interest in the study of *nonlinear surface waves* has been renewed after the theoretical prediction [5] and subsequent experimental demonstration [6] of nonlinearity induced light localization near the edge of a one-dimensional waveguide array with self-focusing nonlinearity that can lead to the formation of the so-called nonlinear Tamm states or *surface solitons*. The generation of such a surface soliton can be understood with the help of simple physics [7] as a trapping of a discrete soliton [8] near the repulsive edge of the truncated lattice when the beam power exceeds some threshold value. These surface solitons become possible solely due to discreteness effects, and they exist in neither continuous nor linear limits. Some of the specific features of such optical surface solitons in other relevant physical settings have been recently investigated both theoretically [9–12] and experimentally [13–15].

Recently, it was shown theoretically that magnetic metamaterials composed of split-ring resonators may exhibit discreteness effects due to weak coupling [16,17]. In particular, it was shown that in one-dimensional discrete arrays of nonlinear split-ring resonators (SRRs), where each ring interacts with its nearest neighbors, on-site nonlinearity [18] and weak coupling [16,17] may result in the appearance of discrete breather excitations, both in the energy conserved and the dissipative system [16]. In nonlinear magnetic metamaterials discrete breathers have been analyzed so far in infinite arrays. In this paper, being encouraged by the recent experiments in optics [6,13–15], we study the discrete breathers located near the edge of a one-dimensional discrete array of nonlinear SRRs. We demonstrate the existence of a class of nonlinear surface localized states, the so-called surface breathers, which exhibit features that have no counterpart in the continuous limit. Actually, a two-dimensional magnetic metamaterial comprised of SRRs with varactor diodes, which makes it nonlinear, has been already realized [19]. That metamaterial, which operates at microwave frequencies, is dynamically tunable by varying the amplitude of the propagating electromagnetic waves.

We consider a periodic array of identical nonlinear SRRs, which is a simple realization of a magnetic metamaterial in one dimension, with the SRRs separated by distance d. Two different configurations, planar and axial, are shown schematically in Figs. 1(a) and 1(b), respectively. In the planar configuration, all SRR loops are lying in the same plane with their centers located on a straight line, while in the axial configuration the line connecting the centers of the SRR loops is perpendicular to the plane of the loops. Each SRR can be mapped to a nonlinear resistor-inductor-capacitor circuit featuring self-inductance L, ohmic resistance R, and capacitance C. We assume that the SRRs become nonlinear due to a Kerr-type dielectric filling their slits [18]. The field-dependent permittivity of that dielectric is of the form $\epsilon(|\mathbf{E}|^2)=\epsilon_0(\epsilon_\ell+\alpha|\mathbf{E}|^2/E_c^2)$, where $\mathbf{E}$ is the electric field, E_c is a characteristic (large) electric field, ϵ_ℓ is the linear permittivity, ϵ_0 is the permittivity of the vacuum, and $\alpha=+1$ (-1) corresponding to the focusing (defocusing) nonlinearity. As a result, the SRRs acquire a field-dependent capacitance $C(|\mathbf{E}|^2)\propto\epsilon(|\mathbf{E}_g|^2)$, where $\mathbf{E}_g$ is the electric field induced along the SRR slit [18]. The origin of $\mathbf{E}_g$ may be due to the magnetic and/or the electric components of the applied field, depending on the relative orientation of that field with respect to the SRRs' plane and the slits. In the following we assume that, for both configurations, the magnetic component of the incident electromagnetic field is perpendicular to the SRRs'

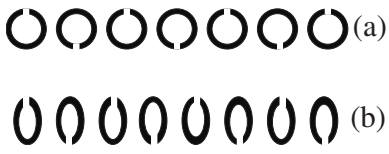

FIG. 1. Schematic of a one-dimensional array of split-ring resonators in (a) planar and (b) axial geometries. The axes of the split-ring resonators as well as the magnetic component of the applied field are directed in parallel. The electric field component is transversal to the slits.

plane, while the electric component is transversal to the slits. Then, only the magnetic component excites an electromotive force, resulting in an oscillating current in each SRR loop. The charge Q in the capacitor of a SRR is given by

$$Q = C_\ell(1 + \alpha U^2/3\epsilon_\ell U_c^2)U, \tag{1}$$

where $U=d_gE_g$, C_ℓ is linear capacitance, and $U_c=d_gE_c$, d_g being the size of the slits. The SRRs in an array are coupled together due to magnetic interaction through their mutual inductances, with nearest-neighbor coupling.

The dynamics of the charge Q_n accumulated in the capacitor of the nth SRR, if one ignores ohmic losses, is described by the equation [16,17,20]

$$L\frac{d^2}{dt^2}\{\lambda Q_{n-1} + Q_n + \lambda Q_{n-1}\} = -f(Q_n), \tag{2}$$

where $\lambda=L/M$ describes the coupling between the neighboring SRRs with the mutual inductance M, and $f(Q_n)=U_n \equiv U(Q_n)$ is found from Eq. (1). The current I_n in the nth SRR is defined as $I_n=dQ_n/dt$. Equation (2) can be written in the normalized form as

$$\frac{d^2}{d\tau^2}\{\lambda q_{n-1} + q_n + \lambda q_{n+1}\} = -f(q_n), \tag{3}$$

where we use the following scaling: $\omega_\ell^{-2}=LC_\ell$, $\tau=t\omega_\ell$, $I_c=U_c\omega_\ell C_\ell$, $Q_c=C_\ell U_c$, $I_n=I_c i_n$, and $Q_n=Q_c q_n$. Equation (3) can be derived from the Hamiltonian

$$\mathcal{H} = \frac{1}{2}\sum_n \{\dot{q}_n^2 + \lambda\dot{q}_n(\dot{q}_{n-1} + \dot{q}_{n+1})\} + \sum_n V_n, \tag{4}$$

where the first (second) term represents the "kinetic" (potential) energy. The nonlinear on-site potential V_n is given by

$$V_n \equiv V(q_n) = \int_0^{q_n} f(q_n')dq_n', \tag{5}$$

and $\dot{q}_n \equiv dq_n/d\tau$. The function $f(q_n)$ can be approximated by the series $f(q_n) \simeq q_n - \chi q_n^3 + 3\chi^2 q_n^5 - \cdots$, where $\chi=\alpha/3\epsilon_\ell$.

The on-site potential Eq. (5) with the exact form of $f(q_n)$ (not given here) can be calculated analytically. For example, for $\alpha=+1$ that potential is of the form

$$V_n = b_0 g^{2/3} + b_1 g^{-4/3} + b_2 g^{4/3} + b_3 g^{-2/3} + \frac{1}{6\chi}, \tag{6}$$

where

$$g = -9q_n\chi^2 + \sqrt{3}g_1, \quad g_1 = \sqrt{(4 + 27\chi q_n^2)\chi^3}, \tag{7}$$

and b_0, b_1, b_2, b_3 are constants

$$b_0 = -3^{1/3}/(6^{5/3}\chi^2), \quad b_1 = +3^{1/3}\chi/6^{2/3}, \tag{8}$$

$$b_2 = +2^{1/3}/(24\cdot 6^{2/3}\chi^3), \quad b_3 = -2^{1/3}/6^{2/3}. \tag{9}$$

A similar expression can be obtained for the case $\alpha=-1$.

We consider two different configurations of one-dimensional SRR arrays shown in Fig. 1, with the same number of SRR oscillators $N=50$. Within the equivalent circuit model, the difference between the two configurations resides in the sign and the magnitude of the coupling parameter λ. Specifically, in the planar (axial) configuration λ is negative (positive).

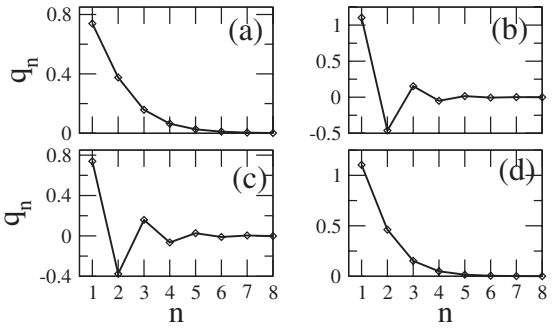

FIG. 2. Profiles of nonlinear surface breathers in an SRR array for (a),(b) planar and (c),(d) axial geometries, with $\epsilon_\ell=2$, $N=50$, and (a) $\alpha=-1$, $\lambda=-0.035$, $T_T=6.69$, (b) $\alpha=+1$, $\lambda=-0.04$, $T_T=6.69$ (c) $\alpha=-1$, $\lambda=0.035$, $T_T=5.95$, and (d) $\alpha=+1$, $\lambda=0.04$, $T_T=5.95$.

For the Hamiltonian system (3), surface states can be constructed with the same methods used for the construction of Hamiltonian discrete breathers, i.e., starting from the anticontinuous limit [21] where all SRRs are uncoupled ($\lambda \to 0$). Here we are interested in finite SRR arrays with open-ended boundary conditions, i.e.,

$$q_0 = 0, \quad q_{N+1} = 0. \tag{10}$$

A surface localized state of the one-dimensional system obviously corresponds to an edge state, i.e., a state with a maximum at either the first or the last element of the array, which decays quickly away from the array edge. According to Ref. [21] we first identify the period T_T of a state with given amplitude q_T for a single array element. Then, for the whole array, an initial condition with $q_n=0$ for any $n\neq 1$, $q_1=q_T$, and $\dot{q}_n=i_n=0$ for any n represents a trivial surface state (surface breather) with period T_T and $\lambda=0$. Continuation of this solution for $\lambda\neq 0$ using the Newton's method results in numerically exact surface breathers up to some maximum value of the coupling parameter $\lambda=\lambda_{max}$. The requirement for the existence of such states is that their frequency $\Omega_T=2\pi/T_T$ and all its multiples lie outside the linear dispersion band $\Omega_\kappa=1/\sqrt{1+2\lambda\cos(\kappa)}$, where $\Omega=\omega/\omega_\ell$ is the normalized frequency, and $\kappa=kd$ is the normalized wave number ($-\pi\leq\kappa\leq\pi$). They should cease to exist when the linear wave band, which expands with increasing λ, reaches the excitation frequency Ω_T. That will occur at $|\lambda|=|\lambda_{max}|=|1-1/\Omega_T^2|/2$.

Following the procedure described above, we have constructed several types of highly localized surface breathers in both the planar and axial configurations, and both self-focusing ($\alpha=+1$) and self-defocusing ($\alpha=-1$) nonlinearities. The profiles of such states, i.e., the normalized charge q_n as a function of the array site n, taken at maximum amplitude, are shown in Figs. 2(a)–2(d). The staggered and/or unstaggered character of those states depends on the combination of the signs of the coupling λ and the nonlinearity coefficient α. Specifically, they are staggered for $\alpha\lambda<0$ [see Figs. 2(b) and

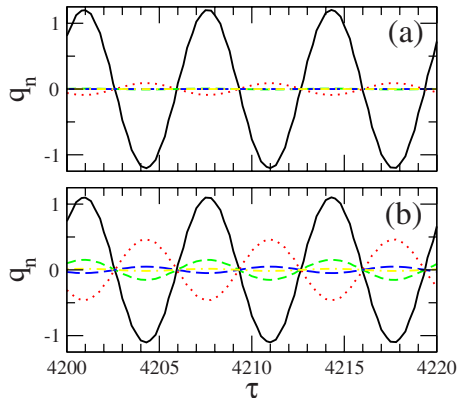

FIG. 3. (Color online) Time evolution of q_n, $n=1,2,3,4,5$, of the nonlinear Tamm states in a SRR array in the planar geometry for $\alpha=+1$, $\epsilon_\ell=2$, $T_T=6.69$, and $\lambda=-0.02$ (a); $\lambda=-0.04$ (b). In this figure q_1 is black solid, q_2 is red dotted, q_3 is green dashed, q_4 is blue long-dashed, and q_5 is yellow dotted-dashed.

2(c)] and unstaggered for $\alpha\lambda>0$ [see Figs. 2(a) and 2(d)]. Multiple-site surface breathers can be also constructed with Newton's method, with appropriate choice of the initial conditions.

Since the system is one dimensional, there is no possibility for transverse motion. However, the surface breathers have their own internal dynamics since, similar to their bulk counterparts, they execute periodic oscillations with frequency Ω_T. A typical example of the time evolution of the q_n's for the first few sites is shown in Fig. 3. In this specific case the time dependence of q_n's is almost sinusoidal. This need not necessarily be true for other parameter sets. Here also the staggered character of that specific state is revealed, since neighboring q_n's oscillate with opposite phases.

Furthermore, surface breathers having their maxima located at sites other than the first one can be constructed, as shown in Fig. 4. In this figure, surface breather profiles are located either at $n=1$ (true surface breathers) or at $n=2$ and $n=3$. The states in Figs. 4(b) and 4(c) [Figs. 4(e) and 4(f)]

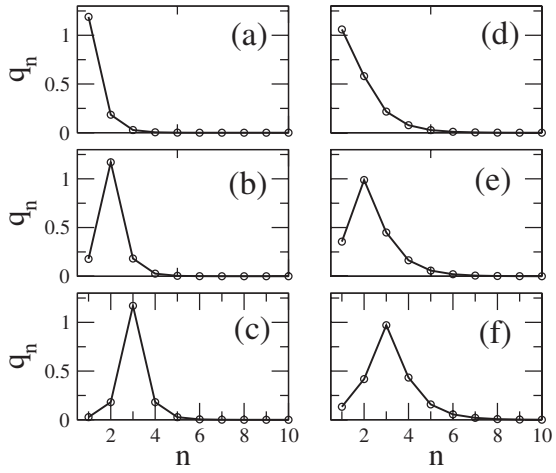

FIG. 4. Profiles of the nonlinear surface states near the edge of the truncated SRR array in the axial geometry ($\lambda>0$) for $\alpha=+1$, $\epsilon_\ell=2$, $T_T=6.69$, $N=50$, and (a)–(c) $\lambda=0.02$ and (d)–(f) $\lambda=0.043$. The states are located at (a),(b) $n=1$, (c),(d) $n=2$, and (e),(f) $n=3$.

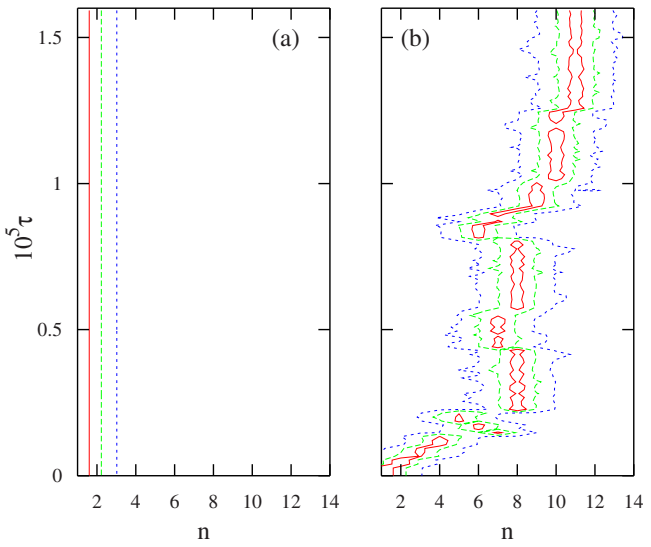

FIG. 5. (Color online) Energy density E_n on the n-τ plane for nonlinear surface breathers for $\alpha=+1$, $\epsilon_\ell=2$, $T_T=6.69$, $N=50$, followed for $24000T_T$, and (a) $\lambda=0.0426$, stable state; (b) $\lambda=0.0428$, unstable state. Contour levels at 0.3 (solid red curves), 0.12 (green dashed curves), and 0.02 (blue short-dashed curves).

describe a crossover regime between the state in Fig. 4(a) [Fig. 4(d)], with the maximum amplitude at the surface, and the states with a maximum at larger n ($n>3$, bulk breathers), which are weakly affected by the presence of the surface.

In comparison with the infinite SRR array, the truncated array introduces an effective repulsive potential at the surface, which is combined with the periodic (Peierls-Nabarro) potential of the infinite array (see also Ref. [7]). As a result, surface breathers cannot exist in the linear regime or in the continuous limit. The surface breathers become unstable well before their frequency touches the linear wave band. At some critical value of $|\lambda|=|\lambda_c|<|\lambda_{max}|$ the repulsion from the surface exceeds the Peierls-Nabarro potential for this $|\lambda_c|$, resulting in the transformation of the surface state to a discrete soliton (breather) which moves irregularly in the SRR lattice. An illustrative example of such behavior is shown in Fig. 5. There the time evolution of the energy density of the SRR array is plotted for two different values of λ around the instability threshold for a specific set of parameters. While in Fig. 5(a) the energy is clearly localized at the edge of the array, remaining constant for long time intervals, in Fig. 5(b) the surface breather is transformed into an irregularly moving discrete breather. However, even that wandering discrete breather seems to be rather long-lived, while its total energy remains constant.

Figure 6 shows the total energy E_{tot} given by the Hamiltonian (4) of the localized surface breathers shown in Figs. 4(a)–4(c) for which $\lambda=0.02$ [Fig. 6(a)], as well as for the corresponding states for $\lambda=0.03$ [Fig. 6(b)], as a function of their frequency Ω_T. We observe that there is an excess of energy for the true surface breathers compared to the crossover cases and of course the bulk breathers. This energy difference increases with increasing λ, as can be inferred by direct comparison between Figs. 6(a) and 6(b). The total energy decreases almost linearly with increasing frequency Ω_T.

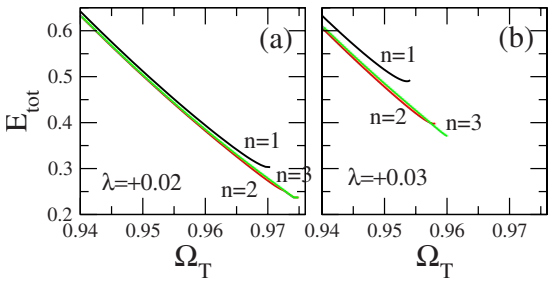

FIG. 6. (Color online) Energy of the nonlinear surface states as a function of Ω_T near the edge of the truncated SRR array in the axial geometry for $\alpha=+1$, $\epsilon_\ell=2$, $N=50$, and λ as shown in the figure. The state at $n=1$ is located at the edge and it has the maximum energy.

The E_{tot}-Ω_T curves begin to curve at relatively high frequencies and eventually show an up turn when the surface breathers become unstable. The critical frequency, defined by $dE_{tot}/d\Omega_T=0$, clearly depends on the coupling parameter λ and the location of the maximum amplitude of the surface states. The qualitative aspects of Fig. 6 are similar to those of the corresponding figures of power vs propagation constant for surface states in the semi-infinite waveguide arrays [7].

In conclusion, we have analyzed the effect of boundaries on the properties of discrete breathers in arrays of nonlinear split-ring resonators. We have demonstrated that near the edge of the array, on-site magnetic nonlinearity and discreteness may support a class of nonlinear surface localized states, the so-called surface breathers, which exhibit features that have no counterparts in the continuous limit and, in particular, exist above a certain energy threshold. We have studied a crossover between nonlinear surface states and discrete breathers by analyzing the families of odd and even modes centered at finite distances from the surface. Those states, as well as other nonlinear excitations, could be created in metamaterials similar to the one presented in Ref. [19]. In the present work we study the surface states in the ideal case where there are no losses. In the presence of losses, we should also analyze their relaxation in finite lifetime, or the convergence of an "arbitrary state" to a surface state. However, we may expect that in the presence of pumping or gain the driven state would be close to the undamped state that we study, but with the parameters defined by a balance of gain and loss.

This work was supported in part by the Australian Research Council through the Discovery Project. One of us (G.P.T.) acknowledges support by the Discovery Project and the Nonlinear Physics Center at the Australian National University, where part of the work was done, for its hospitality.

[1] I. Tamm, Phys. Z. Sowjetunion **1**, 733 (1932).
[2] W. Shockley, Phys. Rev. **56**, 317 (1939).
[3] A. A. Maradudin and G. I. Stegeman, in *Surface Phonons*, edited by W. Kress and F. W. De Wette (Springer-Verlag, Berlin, 1991), pp. 5–35.
[4] V. M. Agranovich and D. L. Mills, *Surface Polaritons* (North Holland, Amsterdam, 1984).
[5] K. G. Makris, S. Suntsov, D. N. Christodoulides, G. I. Stegeman, and A. Haché, Opt. Lett. **30**, 2466 (2005).
[6] S. Suntsov, K. G. Makris, D. N. Christodoulides, G. I. Stegeman, A. Haché, R. Morandotti, H. Yang, G. Salamo, and M. Sorel, Phys. Rev. Lett. **96**, 063901 (2006).
[7] M. I. Molina, R. A. Vicencio, and Yu. S. Kivshar, Opt. Lett. **31**, 1693 (2006).
[8] See Yu. S. Kivshar and G. P. Agrawal, *Optical Solitons: From Fibers to Photonic Crystals* (Academic Press, San Diego, 2003), and references therein.
[9] Y. V. Kartashov, L. Torner, and V. A. Vysloukh, Opt. Lett. **31**, 2595 (2006).
[10] Y. V. Kartashov, F. Ye, V. A. Vysloukh, and L. Torner, Opt. Lett. **32**, 2260 (2007).
[11] Y. V. Kartashov, V. A. Vysloukh, and L. Torner, Phys. Rev. A **76**, 013831 (2007).
[12] M. I. Molina, Y. V. Kartashov, L. Torner, and Yu. S. Kivshar, Opt. Lett. **32**, 2668 (2007).
[13] C. R. Rosberg, D. N. Neshev, W. Krolikowski, A. Mitchell, R. A. Vicencio, M. I. Molina, and Yu. S. Kivshar, Phys. Rev. Lett. **97**, 083901 (2006).
[14] E. Smirnov, M. Stepić, C. E. Rütter, D. Kip, and V. Shandarov, Opt. Lett. **31**, 2338 (2006).
[15] B. Alfassi, C. Rotschild, O. Manela, M. Segev, and D. N. Christodoulides, Phys. Rev. Lett. **98**, 213901 (2007).
[16] N. Lazarides, M. Eleftheriou, and G. P. Tsironis, Phys. Rev. Lett. **97**, 157406 (2006).
[17] I. V. Shadrivov, A. A. Zharov, N. A. Zharova, and Y. S. Kivshar, Photonics Nanostruct. Fundam. Appl. **4**, 69 (2006).
[18] A. A. Zharov, I. V. Shadrivov, and Y. S. Kivshar, Phys. Rev. Lett. **91**, 037401 (2003).
[19] I. V. Shadrivov, A. B. Kozyrev, D. van der Weide, and Y. S. Kivshar, e-print arXiv:0805.0028v1.
[20] M. Eleftheriou, N. Lazarides, and G. P. Tsironis, Phys. Rev. E **77**, 036608 (2008).
[21] J. L. Marín and S. Aubry, Nonlinearity **9**, 1501 (1996).